HTML ABSTRACT + LINKS

Fabrication and morphology of porous *p*-type SiC

Y. Shishkin[a]
Department of Physics and Astronomy, University of Pittsburgh, Pittsburgh, Pennsylvania 15260 and Electrical Engineering Department, University of South Florida, Tampa, Florida 33620

Y. Ke, R. P. Devaty, and W. J. Choyke
Department of Physics and Astronomy, University of Pittsburgh, Pittsburgh, Pennsylvania 15260

(Received 28 May 2004; accepted 17 November 2004; published online 24 January 2005)

Porous silicon carbide fabricated from *p*-type 4H and 6H SiC wafers by electrochemical etching in hydrofluoric electrolyte is studied. An investigation of the dependence on wafer polarity reveals that pore formation is favored on the C face while complete dissolution occurs on the Si face. When the etching is done on the C face, the pore wall thickness decreases with increasing current density. The morphology of the front surface of the sample depends on the prior treatment of the workpiece surface. The porosity is estimated based on the analysis of scanning electron microscope images, charge-transfer calculations, and gravimetric analysis. © *2005 American Institute of Physics*. [DOI: 10.1063/1.1849432]

I. INTRODUCTION

The last decade has enjoyed a rapid and fruitful development of silicon carbide, an indirect wide-band-gap semiconductor whose mechanical and electrical properties are superior to silicon in many respects. Chemical inertness is another property of SiC potentially useful for biological and various sensor applications. At temperatures below a few hundred °C, none of the known etchants for silicon are found to chemically attack SiC at room temperature. Faust, Jr. summarized the reagents which etch SiC at temperatures near 1000 °C.[1] He also reported on the electrolytic dissolution of SiC carried out at room temperature.

There have been a large number of reports on porous *p*-type silicon (see, for example, Ref. 2 for a review), which exhibits a variety of porous structures produced under various anodization conditions. A report on porous *p*-type 6H silicon carbide was published about ten years ago by Shor *et al.*[3] Since then studies of porous SiC have mostly been restricted to electrochemical etching of *n*-type material primarily due to the availability of both 6H and 4H *n*-type wafers. In this work, we undertake a study of the fabrication and properties of porous structures formed from *p*-type SiC wafers. Porous *p*-type SiC has already been applied to Brillouin scattering studies of surface acoustic waves in SiC (Ref. 4) and in protein dialysis experiments.[5] Other potential applications for *p*-type porous SiC include the fields of bone tissue engineering and fuel cells.

II. EXPERIMENT

The electrochemical etching experiments are performed on vicinal carbon basal planes of 6H SiC *p*-type crystals doped to about 2×10^{18} cm^{-3}. In order to study the anodization of surfaces with different degrees of surface finishing, some samples were mechanically polished with diamond paste down to 1 μm mesh, and some with 1/4 μm diamond. Other samples were finished, as a final step, with chemical-mechanical polishing (CMP).

The porous etching is conducted anodically in a 10% hydrofluoric (HF) aqueous solution mixed with ethanol (2:1 measured by weight). A standard three-electrode electrochemical cell configuration is used in which SiC crystals serve as the working electrodes. The electrical current density was set between 0.5 and 60 mA/cm^2. The forward biases applied to the working electrode ranged from 2.0 to 2.5 V.

After etching, samples are carefully removed from the bath and thoroughly washed in acetone and trichloroethylene to remove the residues of black wax used for masking purposes. The gravimetric measurements, conducted prior to and after the etching, are made using a microbalance instrument having a precision of 1 μg. This allows us to determine the weight loss over the course of the etching process. Images of porous structures are obtained in both plan view and cross section for analysis using a Philips XL30 FEG scanning electron microscope (SEM) with a 5-nm spatial resolution.

III. RESULTS AND DISCUSSION

Figure 1 shows rectifying current–voltage characteristics of *p*-type 6H SiC in aqueous HF electrolyte. Since the basal plane of 6H SiC is polar, the (0001), i.e., Si face, and the $(000\bar{1})$, i.e., C face, surfaces are measured separately. The $j(V)$ curve of the Si face has a slightly higher slope than that of the C face above the threshold. However, the slopes are comparable beyond a 2-V bias. The onsets for intense electrochemical etching are about 0.6 V apart indicating that the effective potential barrier for hole transfer across the semiconductor/electrolyte interface is 0.6 V smaller for the carbon face. At a forward bias of about 2 V, the current densities are similar and are on the order of 0.1 mA/cm^2.

Unlike in *p*-type Si, for which the value of the current density determines the porous formation and electropolishing

[a]Electronic mail: shishkin@eng.usf.edu

 © 2005 American Institute of Physics

Downloaded 09 Apr 2006 to 136.142.113.16. Redistribution subject to AIP license or copyright, see http://jap.aip.org/jap/copyright.jsp

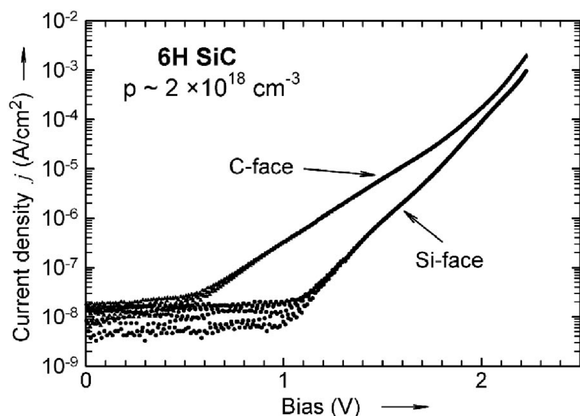

FIG. 1. Typical current density $j(V)$ vs bias voltage characteristics of the C face and Si face of the basal plane of 6H SiC collected in 10% HF aqueous solution with 5% ethanol. Each of the two curves represents a single scan with increasing bias. The data points below the current onsets are instrumental noise.

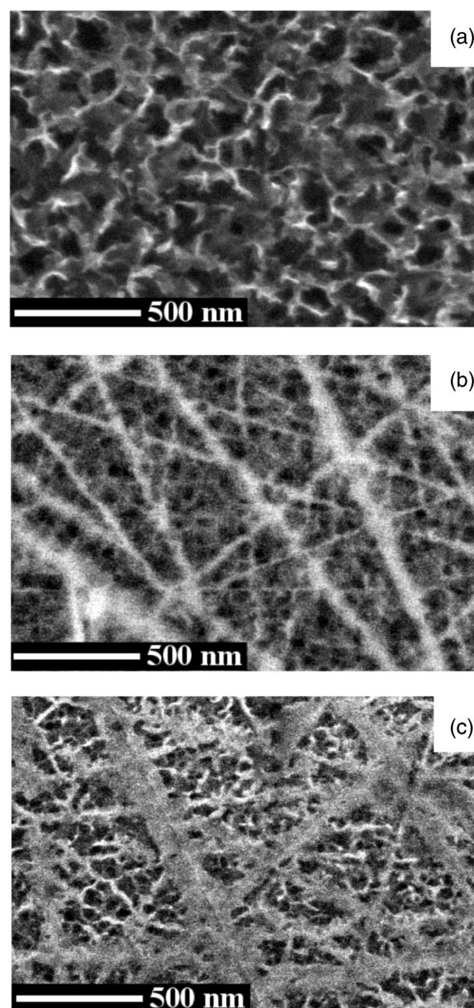

FIG. 2. Plan view SEM images of porous p-type ($p \sim 2.0\times10^{18}$ cm^{-3}) C-face 6H SiC samples treated differently prior to electrochemical etching by (a) chemical-mechanical polishing, (b) diamond paste polishing down to 0.25 μm, and (c) diamond paste polishing down to 1.0 μm.

(i.e., complete dissolution) regimes,[6] one of the major criteria for the formation of a porous structure in p-type SiC is the correct choice of the substrate polarity. When the Si face of a p-type SiC sample is exposed to the anodizing conditions, electropolishing of the crystal occurs for HF concentrations in the range from 1% to 20% (the tested range of concentrations). In contrast, porous structures are formed on the C face provided the HF concentration exceeds 1%. At 1% or below, complete dissolution of the crystal takes place even for C-face crystals.

It is known that the wet oxidation of the (0001) surface, or Si-terminated surface of SiC, proceeds at a much slower rate than that of the $(000\bar{1})$ surface.[7] Our own experiments (unpublished) with wet oxidation of polar SiC surfaces concur with the results obtained in Ref. 7. Since pores form by an oxidation of the surface atoms with the immediate removal of the oxidized species into the electrolytic solution, we speculate that the origin of the difference in the $j(V)$ characteristics as well as the pore formation properties of the two polar surfaces of p-type SiC are likely related to differences in the oxidation properties of the carbon-rich and silicon-rich surfaces.

Figure 2 shows plan view SEM images of the surfaces of p-type SiC, C-face samples, which were treated differently prior to electrochemical etching. The CMP processing was used to pretreat the surface of the sample in Fig. 2(a). One can see that after the anodization, the surface is rough and seems to be the result of randomly positioned pore nucleation sites. This relative susceptibility of the CMP-treated p-type SiC $(000\bar{1})$ face to electrolytic attack is in contrast to the results obtained on surfaces of n-type SiC. After preprocessing with CMP, the surfaces of n-type SiC show strong resistance to electrochemical etching.[8]

The sample shown in Fig. 2(b) was polished with diamond paste prior to anodization. The size of the polishing diamond particles was 0.25 μm. It can be seen that the bulk porous network is overlaid by undissolved surface structures of roughly 50–100 nm in width, roughly corresponding to a quarter of the 0.25-μm size diamond particles. Since the average width of a scratch on a polished surface is in practice thought to be approximately one-fourth of the size of a particle of the polishing agent, we presume that the etched p-type SiC C-face surfaces are comprised of etch-resistant structures associated with the scratches left after the mechanical polishing. This is supported by Fig. 2(c), which shows a plan view image of a porous sample whose front surface was polished prior to etching with diamond paste down to 1 μm. One can see that the dominating surface fiber width has increased to 100–200 nm. In fact, other samples exhibited surface features up to 500 nm in width (not shown). The experiments with etching surfaces on n-type SiC demonstrate that surface scratches in this material result in an opposite effect compared to what is seen in Figs. 2(b) and 2(c), i.e., surface pore nucleation is favored by damage created by mechanical polishing in n-type SiC (Fig. 3).

CMP processing, as compared to mechanical polishing, is known to produce damage-free surfaces of SiC.[9] Although the technology of CMP for C-face p-type SiC has not been fully developed yet, the front surface roughness of our CMP-processed samples is in the range of 10–30 Å rms, as measured by atomic force microscopy (AFM). More importantly,

Downloaded 09 Apr 2006 to 136.142.113.16. Redistribution subject to AIP license or copyright, see http://jap.aip.org/jap/copyright.jsp

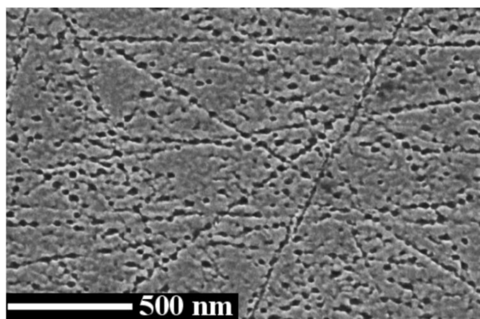

FIG. 3. Plan view SEM image of porous *n*-type C-face 4H SiC whose front surface was polished with 0.25-μm diamond paste prior to electrochemical etching.

the front surface is scratch-free, which is a definite improvement as compared to the surfaces polished with 0.25-μm diamond paste. Therefore, based on Fig. 2, we conclude that scratches associated with mechanical polishing are resistant to electrochemical etching in *p*-type silicon carbide.

Figure 4(a) shows a cross-sectional SEM image of a bulk porous morphology obtained in a C-face sample (original substrate doping is $p \sim 2.4 \times 10^{18}$ cm^{-3}) at a current density of 1.0 mA/cm^2. The porous film growth rate, which can be roughly defined as the ratio of the film thickness to the total etching time, is fairly low, less than 1 μm/h at this current density. The estimated thickness of the pore walls under these conditions ranges from 15 to 40 nm. The observed *branched*-type of morphology is typical for our highly doped *p*-type C-face 6H SiC samples anodized at current densities up to 15 mA/cm^2. Although the morphology does not change, the thickness of the pore walls diminishes with increasing current density, reaching 5–15 nm for samples etched at 15 mA/cm^2. The forward bias required to achieve reasonable dissolution rates varies between 2.0 and 2.5 V.

When the current density is increased above 15 mA/cm^2, the morphology has the appearance of a *filamentary* structure, as seen in Fig. 4(b). The sample shown in Fig. 4(b) was etched at a current density of 30 mA/cm^2. The resolution of our SEM instrument does not allow us to accurately measure the size of the structures in the filamentary morphology. However, we estimate the pore wall thickness to diminish to the 1-nm range. This result agrees with the interpore spacing obtained in Ref. 3 by transmission electron microscope (TEM) analysis. In Ref. 3, a current density of 50 mA/cm^2 was used.

Despite the observed dependence of the interpore spacing on the dissolution current, there are general similarities for all *p*-type C-face SiC porous samples. First, unlike porous *p*-type Si, we have not observed any indication of preferential etching along specific crystallographic directions. One exception is the ⟨0001⟩ direction along which complete crystal dissolution occurs. To demonstrate that etching in *p*-type SiC is indeed independent of orientation, an experiment should be carried out in which a nonbasal plane surface of SiC undergoes anodization. Second, the porosity P, defined as the ratio of the volume of the void space V_p to the total volume V, is uniform throughout the porous film. A porosity gradient is typically observed for *n*-type SiC samples, for which the formation of the porous structures is facilitated by front surface UV illumination. In this case, optically generated holes, required for the etching process, are minority carriers, contrary to the holes in *p*-type material, which are the majority carriers.

The uniform etching [no porosity gradient seen in Figs. 4(a) and 4(b)] of *p*-type SiC makes it possible to derive a simple relationship for porosity P depending on the anodization current density. Let us call γ the number of holes required to dissolve a single Si–C pair. Shor and Kurtz[10] reported that carbon dioxide (CO_2) and carbon monoxide (CO) bubbles were observed during the electrochemical etching of 6H SiC in HF. Assuming that no SiO and SiO_2 are present in the HF aqueous solution and taking into account that anodic etching of silicon in aqueous HF produces stable SiF_6^{2-} ions,[11] we propose the following overall reactions:

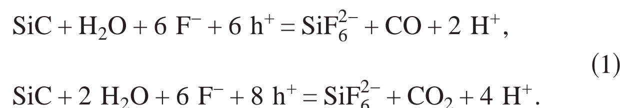

$$\mathrm{SiC} + \mathrm{H_2O} + 6\ \mathrm{F^-} + 6\ \mathrm{h^+} = \mathrm{SiF_6^{2-}} + \mathrm{CO} + 2\ \mathrm{H^+},$$
$$\mathrm{SiC} + 2\ \mathrm{H_2O} + 6\ \mathrm{F^-} + 8\ \mathrm{h^+} = \mathrm{SiF_6^{2-}} + \mathrm{CO_2} + 4\ \mathrm{H^+}. \quad (1)$$

These electrochemical reactions do not account for the possibility of reaction steps described by partial reactions.

From (1), the range of values for the parameter γ is from 6 to 8. A value of 6.9 has been obtained for the dissolution of *n*-type 6H SiC.[10] Recently, we began systematic gravimetric measurements to determine the value of this parameter using a sensitive microbalance. Preliminary data obtained using both 6H and 4H SiC show that γ for *p*-type SiC may be polytype dependent and decreases for higher current densities. We observe a value of γ close to 6 at current densities on the order of 1 mA/cm^2, which decreases to 5 or lower for current densities above 10 mA/cm^2. We suggest two possible explanations for the observed tendency. First, the reac-

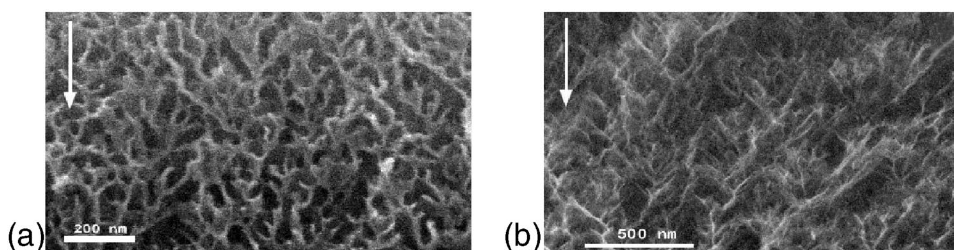

FIG. 4. Cross-sectional SEM image of a porous *p*-type ($p \sim 2.4 \times 10^{18}$ cm^{-3}) C-face 6H SiC sample electrochemically etched at (a) about 1.0 mA/cm^2 (the pore wall thickness is 15–40 nm) (b) about 30.0 mA/cm^2 (the pore wall thickness is 1–15 nm). Note the different scale bars in Figs. 4(a) and 4(b) The arrows indicate the etching direction.

Downloaded 09 Apr 2006 to 136.142.113.16. Redistribution subject to AIP license or copyright, see http://jap.aip.org/jap/copyright.jsp

tions in (1) may not necessarily occur at equal rates, with the first reaction dominating over the second one. Second, if there is some hydrogen (H_2) evolution at higher currents instead of just hydrogen ions H^+ dissolved in the solution, for example,

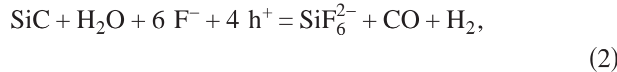

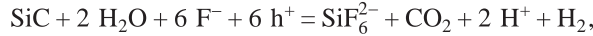

$$\begin{aligned} &SiC + H_2O + 6\ F^- + 4\ h^+ = SiF_6^{2-} + CO + H_2, \\ &SiC + 2\ H_2O + 6\ F^- + 6\ h^+ = SiF_6^{2-} + CO_2 + 2\ H^+ + H_2, \end{aligned} \tag{2}$$

there will be less positive charge required [4 and 6, respectively, for the reactions in (2)] to dissolve a Si–C pair. In such a case, γ will be smaller. Sample doping may also affect the value of γ.

The number of holes participating in the dissolution reactions during time dt is dQ/e, where dQ is the charge transferred across the semiconductor/electrolyte interface. The corresponding number of dissolved Si–C pairs is

$$dN = \frac{dQ}{e\gamma}. \tag{3}$$

Knowing the exposed front surface area A and assuming that we know the uniform current density $j(t)$, we can write

$$dQ = j(t)A dt. \tag{4}$$

Therefore, if V_0 is the volume occupied by one Si–C pair, then using (3) and (4), the rate at which SiC volume dissolves is

$$V_0 \frac{dN}{dt} = V_0 \frac{jA}{e\gamma}.$$

Then, the rate at which the crystal volume is made porous is

$$\frac{dV}{dt} = \frac{V_0 jA}{e\gamma P}, \tag{5}$$

where P is the porosity. On the other hand, the same quantity may be written as

$$\frac{dV}{dt} = A \frac{dx}{dt}, \tag{6}$$

where dx/dt is the velocity of propagation of the front separating the porous from the nonporous material. Here, we are making the simplifying assumption that there are two distinct types of uniform material, porous and nonporous, with an abrupt interface, neglecting the details of the development of the porous network. The thickness of the porous/nonporous interface is about 10–20 nm. A comparison to a typical porous film thickness, 1–5 μm, makes the abrupt interface a good approximation. Therefore, using (5) and (6) and canceling the front surface area A, one gets

$$P = \frac{V_0 j}{e\gamma dx/dt}. \tag{7}$$

In order to find the experimental dependence of dx/dt vs j, a few samples were anodized at different etching current densities ranging from about 0.5 to 45 mA/cm^2. The samples were analyzed in cross section with the SEM in order to determine the film thicknesses. Our SEM images show that, once the porous structure formed, the pore wall

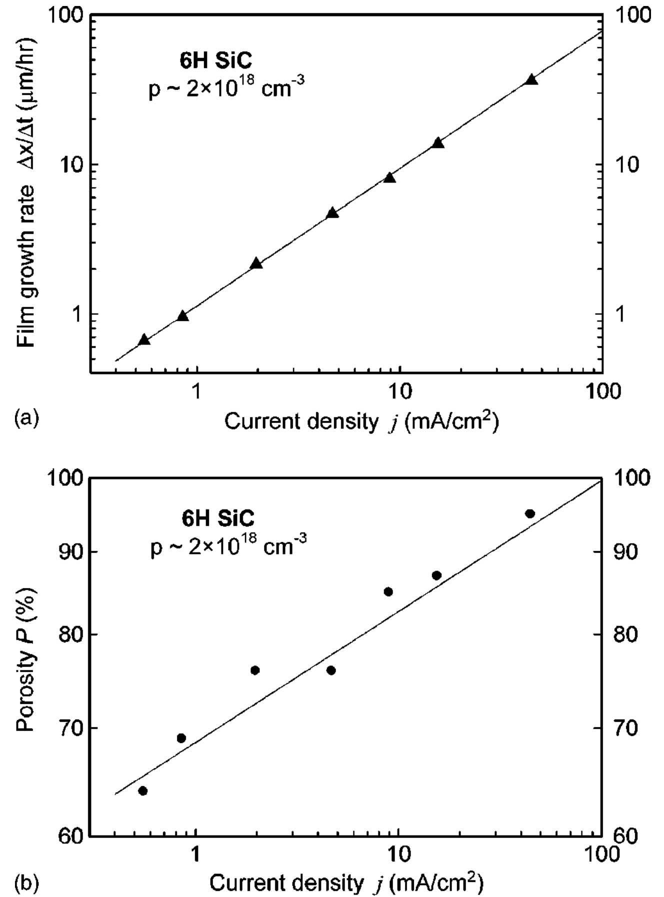

FIG. 5. (a) Experimental dependence of the average speed of the porous film growth in p-type 6H SiC crystals ($p \sim 2 \times 10^{18}$ cm^{-3}) on the applied current density. The electrolyte is aqueous 10% HF mixed with 5% ethanol. The solid line is a fit to $\Delta x/\Delta t = \alpha j^{\beta}$. (b) The calculated porosity based on Eq. (8) with $\gamma = 6$. The solid line is based on the prediction of Eq. (10).

thickness does not change as the etching proceeds. For a given current density, the pore wall thickness is the same from the exposed surface down to the porous/substrate interface indicating that the p-type porous network is inert with respect to further electrochemical dissolution once the front has passed. This implies that the etching proceeds only near the porous/nonporous interface, and that the porosity is uniform and not a function of depth. Note that should the doping of the sample be nonuniform, the porosity is likely to vary with depth. Assuming uniform doping, we can then approximate $dx/dt \approx \Delta x/\Delta t$, where Δx is the film thickness measured by SEM and Δt is the total etching time. Thus using relationship (7) we write

$$P \approx \frac{V_0 j}{e\gamma \Delta x/\Delta t}. \tag{8}$$

Since V_0 is one-sixth of the unit cell of 6H SiC, it can be determined from the lattice constants of 6H SiC [$a = 3.08$ Å and $c = 15.12$ Å (Ref. 12)]. One obtains $V_0 = 20.7 \times 10^{-24}$ cm^3.

Figure 5(a) shows the experimental results for the dependence of the porous film growth rate $\Delta x/\Delta t$ versus current density j. If the data in Fig. 5(a) are fitted to the dimensionless relationship $y(x) = \alpha x^{\beta}$, the coefficients α and β are found to be about 1.13 and 0.92, respectively, implying a

Downloaded 09 Apr 2006 to 136.142.113.16. Redistribution subject to AIP license or copyright, see http://jap.aip.org/jap/copyright.jsp

slightly sublinear dependence. Since we use the nonstandard units, (μm/h) for $\Delta x/\Delta t$ and (mA/cm^2) for j, in the relatioship $(\Delta x/\Delta t)=\alpha j^{\beta}$, the units of α are (μm/h)(mA/cm^2)$^{-\beta}$, while β is dimensionless.

In Fig. 5(b) we plot the porosity P calculated using the obtained experimental data of $\Delta x/\Delta t$ vs j and Eq. (8). Note that we have set $\gamma=6$, which may not be the case for all the samples listed for the reasons discussed earlier. Although an almost linear dependence is observed for $\Delta x/\Delta t$ vs j, one can see that the calculated value of the porosity increases with increasing current density in a nonlinear fashion.

Using $\Delta x/\Delta t=\alpha j^{\beta}$, Eq. (8) may be rewritten as

$$P=\frac{V_0 j}{e\gamma\alpha j^{\beta}}=\frac{V_0 j^{1-\beta}}{e\alpha\gamma}. \tag{9}$$

In order to take into account the nonstandard units, one needs a multiplicative factor 3.6×10^4 in front of the right-hand side of (9). The final expression, which is used to predict the behavior of the points in Fig. 5(b) (solid line), is then

$$P=3.6\times10^4\frac{V_0 j^{0.08}}{1.13e\gamma}\approx0.686j^{0.08}, \tag{10}$$

where j is expressed in mA/cm^2. From this relation, we may estimate that the maximum current density that can be used for Eq. (10) to be valid is about 100 mA/cm^2. The minimum achievable porosity $P_{\min}$ for our apparatus can also be estimated. Using Eq. (10) and the value for the instrumental noise level ($\sim10^{-8}$ A/cm^2; see Fig. 1) for the samples under study, one obtains $P_{\min}=27\%$.

When our microbalance became available, we evaluated the porosity based on the gravimetric analysis. For a 6H SiC $p\sim2\times10^{18}$ cm^{-3} sample etched at a current density of 2.0 mA/cm^2, we measured a loss of 110 µg as a result of 1 h of etching. This corresponds to the void volume inside the SiC crystal $V_p=34\times10^{-6}$ cm^3, given that the mass density of SiC is 3.21 g/cm^3. After the thickness of the porous film was determined by SEM to be 1.9 µm, we experimentally obtained the porosity $P=V_p/V=82\%$ front surface area $\sim$0.21 cm^2. This result is in fair agreement with the value $P=76\%$ obtained for a similar sample, which was etched at about 2.0 mA/cm^2 [see the data in Fig. 5(b)]. The slight disagreement between the two values of porosity for these two similar but distinct samples may originate from the uncertainty in γ and the different values of sample resistivity. The nominal resistivity value (Ω cm) is provided by the manufacturer and is believed to have a 20% error margin over the wafer used for this experiment.

IV. CONCLUSION

We have electrochemically etched p-type 6H silicon carbide in aqueous hydrofluoric acid solution. The etching is done in the anodic regime and results in porous layer formation when performed on the C-face basal plane. A complete dissolution of the crystal structure occurs for the (0001) basal plane, or Si face. In p-type SiC the surface morphology of the porous structure depends on the details of the polishing prior to anodization while the bulk porous structure is independent of the surface treatment. The average pore size does not significantly change with the applied current density up to about 15 mA/cm^2 for our choice of electrolytic solution, while the pore wall thickness decreases with increasing current density. The methods of estimating bulk porosity using a charge-transfer calculation and the gravimetric analysis are found to provide reasonably close results.

ACKNOWLEDGMENTS

We acknowledge the DURINT Program (ONR Grant No. N00014-01-1-0715) for supporting this research. We also thank II-VI, Inc. for the chemical-mechanical polishing.

[1] J. W. Faust, Jr., in *The Etching of Silicon Carbide*, Silicon Carbide Meeting, Boston, MA 1959 (Pergamon, New York, 1960), p. 403.
[2] H. Föll, M. Christophersen, J. Carstensen, and G. Hasse, Mater. Sci. Eng., R. **39**, 93 (2002).
[3] J. S. Shor, L. Bemis, A. D. Kurtz, I. Grimberg, B. Z. Weiss, M. F. MacMillan, and W. J. Choyke, J. Appl. Phys. **76**, 4045 (1994).
[4] G. T. Andrews, M. J. Clouter, B. Mroz, Y. Shishkin, Y. Ke, R. P. Devaty and W. J. Choyke, Mater. Sci. Forum **457–460**, 653 (2004).
[5] A. J. Rosenbloom, Y. Shishkin, D. M. Sipe, Y. Ke, R. P. Devaty, and W. J. Choyke, Mater. Sci. Forum **457–460**, 1463 (2004).
[6] R. L. Smith and S. D. Collins, J. Appl. Phys. **71**, R1 (1992).
[7] A. Rys, N. Singh, and M. Cameron, J. Electrochem. Soc. **142**, 1318 (1995).
[8] R. M. Feenstra (private communication).
[9] S. Monnoye, D. Turover, and P. Vicente, in *Silicon Carbide*, edited by W. J. Choyke, H. Matsunami, and G. Pensl (Springer, Berlin, 2004), p. 699.
[10] J. S. Shor and A. D. Kurtz, J. Electrochem. Soc. **141**, 778 (1994).
[11] V. Lehmann and H. Föll, J. Electrochem. Soc. **137**, 653 (1990).
[12] A. Taylor and R. M. Jones, in *SiC—A High Temperature Semiconductor*, edited by J. R. O'Connor and J. Smiltjens (Pergamon, Oxford, 1960), p. 147.

Downloaded 09 Apr 2006 to 136.142.113.16. Redistribution subject to AIP license or copyright, see http://jap.aip.org/jap/copyright.jsp